

## Articles

---

### Steroid Ring Hydroxylation Patterns Govern Cooperativity in Human Bile Acid Binding Protein<sup>†</sup>

Gregory P. Tochtrop,<sup>‡,§,||</sup> Jamie L. Bruns,<sup>§</sup> Changguo Tang,<sup>‡</sup> Douglas F. Covey,<sup>§</sup> and David P. Cistola<sup>\*,‡</sup>

*Department of Biochemistry and Molecular Biophysics and Department of Molecular Biology and Pharmacology, Washington University School of Medicine, 660 South Euclid Avenue, Campus Box 8231, St. Louis, Missouri 63110*

*Received April 25, 2003; Revised Manuscript Received July 30, 2003*

**ABSTRACT:** Human ileal bile acid binding protein (I-BABP) is a member of the intracellular lipid binding protein family. This protein is thought to function in the transcellular transport and enterohepatic circulation of bile salts. Human I-BABP binds two molecules of glycocholate, the physiologically most abundant bile salt, with modest intrinsic affinity but a remarkably high degree of positive cooperativity. Here we report a calorimetric analysis for the binding of a broad panel of bile salts to human I-BABP. The interaction of I-BABP with nine physiologically relevant derivatives of cholic acid, chenodeoxycholic acid, and deoxycholic acid in their conjugated (glycine and taurine) and unconjugated forms was monitored by isothermal titration calorimetry. All bile salts bound to I-BABP with a 2:1 stoichiometry and similar overall affinity, but the derivatives of cholic acid displayed much higher Hill coefficients, a measure of macroscopic positive cooperativity. To test whether the cooperativity was dependent on individual structural features of the bile salt side chain, a series of side-chain-extended bile salts that lacked a hydrogen bond donor or acceptor at C-24 were chemically synthesized. These synthetic variants exhibited the same energetic and cooperativity profile as the naturally occurring bile salts. Our findings indicate that cooperativity in bile salt–I-BABP recognition is governed by the pattern of steroid B- and C-ring hydroxylation and not the presence or type of side-chain conjugation.

Human ileal bile acid binding protein (I-BABP) is a member of the intracellular lipid binding protein family. This family consists of small proteins (approximately 15 kDa), which are thought to facilitate the cellular and metabolic

trafficking of fatty acids, cholesterol, retinoids, and bile salts (1, 2). Human I-BABP is abundantly expressed in the distal ileocytes of the small intestine and has previously been shown to bind bile salts *in vitro* (3–6). This binding interaction has been implicated to play a role in the enterohepatic circulation of bile salts (7). In addition, I-BABP may play a role in gene regulation by controlling the presentation of bile salts to the farnesyl X receptor (FXR) (8). Hence, understanding the nature of bile salt–I-BABP interactions is important to understanding the physiologic role of I-BABP.

Previously our group has shown that human I-BABP binds two molecules of glycocholate with modest intrinsic affinity

<sup>†</sup> This work was supported by USPHS Grants R01 DK48046 to D.P.C. and GM 47969 to D.F.C. and by the Washington University Digestive Diseases Research Core Center, Grant P30 DK52574.

<sup>\*</sup> To whom correspondence should be addressed. E-mail: cistola@cosine.wustl.edu. Phone: 314-362-4382. Fax: 314-362-4153.

<sup>‡</sup> Department of Biochemistry and Molecular Biophysics, Washington University School of Medicine.

<sup>§</sup> Department of Molecular Biology and Pharmacology, Washington University School of Medicine.

<sup>||</sup> Current address: Institute of Chemistry and Cell Biology, Harvard Medical School, 250 Longwood Ave., SGM 604, Boston, MA 02115.

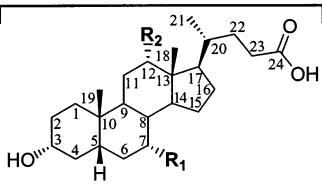
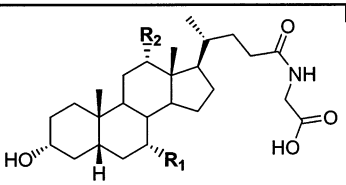
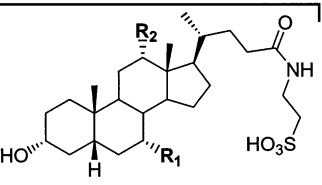
Unconjugated		Glycine Conjugated		Taurine Conjugated	
					
Bile Salt	Abbreviation	R <sub>1</sub>	R <sub>2</sub>	Conjugation	Abundance
Cholic Acid	CA	OH	OH	none	<1 %
Glycocholic Acid	GCA	OH	OH	glycine	40 %
Taurocholic Acid	TCA	OH	OH	taurine	15 %
Chenodeoxycholic Acid	CDA	OH	H	none	<1 %
Glycochenodeoxycholic Acid	GCDA	OH	H	glycine	20 %
Taurochenodeoxycholic Acid	TCDA	OH	H	taurine	5 %
Deoxycholic Acid	DCA	H	OH	none	<1 %
Glycodeoxycholic Acid	GDA	H	OH	glycine	7 %
Taurodeoxycholic Acid	TDA	H	OH	taurine	3 %

FIGURE 1: Nomenclature, structures (including steroid numbering), and relative human abundance of nine physiologically relevant bile salts.

but a remarkably high degree of positive cooperativity (6). The ligand stoichiometry and specificity of I-BABP are unique for this family of proteins. Generally, members of this protein family bind one molecule of ligand, typically a fatty acid or retinoid. The only other family member shown to bind multiple ligands is liver fatty acid binding protein (L-FABP), as illustrated by the X-ray crystal structure of a ternary complex of L-FABP bound to two fatty acids (9). I-BABP is the only member of the family whose primary ligand is bile salts. Its stoichiometry of two bile salts is surprising given the larger molecular dimensions of the steroid framework.

Although glycocholate provided a useful bile salt for initial studies of site-specific binding (6), it did not represent the structural diversity of the bile salt pool in vivo. Shown in Figure 1 is a list of nine physiologically abundant bile salts, which vary with respect to differential hydroxylation patterns of the steroid B- and C-rings and the presence or type of side-chain conjugation. Differential hydroxylation can arise directly from mammalian biosynthesis (cholic acid and chenodeoxycholic acid) or via microbial transformations (10). Deoxycholic acid is an example of a microbial dehydroxylation at C-7 of cholic acid. Conjugation, either to glycine or taurine, lowers the  $pK_a$  and affords compounds that are fully ionized and soluble at physiological pH. Hence conjugated bile salts are more resistant to precipitation by low pH or divalent cations, increasing their effectiveness as detergents. Further, conjugation may prevent passive diffusion of bile salts across cell membranes.

To explore the energetic features of ligand binding, the interactions of human I-BABP with a panel of structurally distinct bile acids were monitored using isothermal titration calorimetry (11). We systematically evaluated four aspects of the bile salt structure as it affected binding to I-BABP. We used this analysis to evaluate the structural contributions to the observed macroscopic binding affinity and cooperativity. These aspects are (1) steroid ring hydroxylation pattern, (2) steroid side-chain conjugation and chemical structure, (3) temperature dependence of cooperativity, and (4) ligand heterogeneity.

We evaluated a panel of naturally occurring bile salts to determine the effects of differential ring hydroxylation and side-chain conjugation on the observed cooperativity. To further examine the energetic role of the bile salt side chain in binding and recognition, a series of bile salt analogues with the side chains elongated by two methylene units were synthesized. Finally, we characterized the binding of mixtures of glycine-conjugated bile salts to human I-BABP. The implications of the observed energetic profiles are discussed.

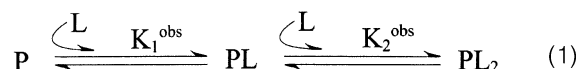
## MATERIALS AND METHODS

**Protein Biosynthesis and Purification.** Recombinant human I-BABP was biosynthesized in *Escherichia coli* and purified to homogeneity as follows. Bacteria harboring the pMON-hIBABP plasmid were grown at pH 7.2 in a New Brunswick Bioflow III high-density fermenter using a nutrient-rich medium containing tryptone (10.8 g/L), yeast extract (22.5 g/L), potassium phosphate (0.1 M), magnesium sulfate (1–5 mM), and calcium chloride (0.1–0.5 mM), as well as trace amounts of iron sulfate and thiamin. Cells were grown to a final density of 55 as monitored by OD<sub>600</sub>. Protein expression, under control of the recA promoter, was induced in mid-log phase by adding nalidixic acid to 100  $\mu$ g/mL. After harvesting, the protein was released from partially lysed cells using a freeze–thaw protocol (12). The cells were suspended in Tris buffer, pH 8.1, containing a broad-spectrum protease inhibitor cocktail (Roche) and were frozen in ethanol/dry ice and thawed. The freeze–thaw cycle was repeated five times. The mixture was subjected to centrifugation (15000g) for 30 min followed by collection of the supernatant, which was then chromatographed on a 25  $\times$  5 cm column of Q-Sepharose Fast Flow. Gel filtration chromatography followed using a 140  $\times$  5 cm column of Sephadex G-50. Complete delipidation was achieved by passing it over a column of lipophilic Sephadex type VI (Sigma product no. H-6258) at 37  $^{\circ}$ C and confirmed by electrospray mass spectrometry. Protein purity, as assessed by overloaded Coomassie-stained SDS–PAGE gels, was >98%. The final yield of purified protein from a 4 L fermentation was approximately 5 g. Protein concentrations were determined

spectrophotometrically as calibrated by quantitative amino acid analysis. A 1 mg/mL solution of human I-BABP in water corresponds to an OD<sub>280</sub> value of 0.846 [for comparison, a value of 0.91 was obtained using composition analysis according to Pace et al. (13)].

**Isothermal Titration Calorimetry.** The calorimetry experiments were performed using a Microcal OMEGA differential titration calorimeter. The *x*-axis discontinuity of all raw data is due to a change in the injection volume from 4 to 7  $\mu$ L. Fifteen injections of 4  $\mu$ L aliquots were followed by 35 injections of 7  $\mu$ L aliquots of 6.50 mM bile salt into a reaction cell containing 1.33 mL of 0.185 mM human I-BABP. In most experiments, the final ligand:protein mole ratio was approximately 6:1. The protein and ligand were dissolved in identical buffers containing 20 mM potassium phosphate, 135 mM KCl, and 10 mM NaCl, pH 7.2. Each titration series was repeated at least three times, with most being repeated five times. The heats of injection were corrected for the heat of dilution of the ligand into buffer and normalized to the amount of bile salt injected.

**ITC Data Fitting.** The ITC data were fit to a stepwise binding model shown diagrammatically as



The stepwise binding model was written in PASCAL, compiled, and then imported as a \*.dll file into the Windows-based nonlinear least-squares analysis program SCIENTIST (Micromath, Inc.). The analysis of the fitted curves yielded the stepwise dissociation constants ( $K_{d1}^{\text{obs}}$ ,  $K_{d2}^{\text{obs}}$ ) and the stepwise binding enthalpies ( $\Delta H_1^{\text{obs}}$ ,  $\Delta H_2^{\text{obs}}$ ). Our group has previously published a mathematical treatment of this model (6).

**Bayesian Data Analysis.** The fitting of the isothermal calorimetry data to the stepwise binding model in eq 1 was assessed using a Bayesian analysis. A Markov chain Monte Carlo method was used to sample 10000 points from the posterior probability distribution of the parameters  $K_{d1}^{\text{obs}}$ ,  $K_{d2}^{\text{obs}}$ ,  $\Delta H_1^{\text{obs}}$ , and  $\Delta H_2^{\text{obs}}$  given the calorimetry data. The last 9000 points were used to obtain the average values of the parameters, and their uncertainties were expressed as one standard deviation. The Markov Chain Monte Carlo sampler was adopted from Radford Neal's software package available at <http://www.cs.toronto.edu/~radford/fbm.software.html>.

## RESULTS

Injection profiles and binding isotherms for the interactions of various bile salts with I-BABP are shown in Figure 2. Bile salts with the same steroid hydroxylation pattern exhibit similar binding profiles irrespective of side-chain conjugation. For example, cholic acid displays the same biphasic profile whether in the unconjugated, glycine-conjugated, or taurine-conjugated form (Figure 2, panels C, E, and G). Likewise, chenodeoxycholic acid displays the same profile whether conjugated or unconjugated (Figure 2, panels D, F, and H). Finally, deoxycholic acid shows the same overall pattern as chenodeoxycholic acid (data not shown). To determine if the similarities in isotherm profile translated to similarities in binding energetics, the ITC data sets were fit

to the stepwise binding model shown in eq 1 using either a nonlinear least-squares or Bayesian analysis. The least-squares analysis yields a single set of parameters with the lowest  $\chi^2$  value. It is therefore possible to underestimate the parameter space consistent with the data. In contrast, the Bayesian analysis gives a distribution of statistically relevant solutions based on the error associated with each raw data point. Further, the Bayesian distribution can be used to directly determine a confidence interval for the binding parameters.

The utility of the Bayesian analysis is well illustrated in the case of taurocholic acid (TCA) as compared to taurochenodeoxycholic acid (TCDA). As seen in Figure 3, the statistically relevant binding parameters for TCA range over >2 orders of magnitude. This problem is especially prevalent when analyzing data from positively cooperative systems where the binding isotherm is dominated by the unligated and doubly ligated states with suppression of the intermediates. In such cases a least-squares analysis can give misleading results. In contrast, the statistically relevant binding parameters for TCDA were much less varied, a reflection of the lower degree of macroscopic cooperativity exhibited by the dihydroxy bile salt derivative.

The binding parameters displayed in Table 1 are the arithmetic mean of a sample of 9000 random points drawn from the posterior distribution as determined by the Bayesian analysis, with the error defined as one standard deviation of the distribution. Note that the overall binding affinities as given by the products of  $K_{d1}^{\text{obs}}$  and  $K_{d2}^{\text{obs}}$  are comparable for the different bile salts. However, the degree of macroscopic cooperativity varies considerably.

A commonly used measuring stick for macroscopic cooperativity is the Hill coefficient. This parameter adopts a value of 1 for a noncooperative system and a maximum value of 2 for a two-site system with infinite positive cooperativity. The most striking pattern in the bile salt binding parameters in Table 1 is the correlation of Hill coefficients with the hydroxylation pattern of the bile salt steroid rings. The trihydroxycholic acid derivatives display the highest degree of macroscopic positive cooperativity with Hill coefficients ranging from 1.86 to 1.91. By contrast, dihydroxy-CDA and DCA derivatives display considerably less cooperativity with Hill coefficients ranging from 1.14 to 1.42.

**Temperature Dependence of Cooperativity.** To address whether the observed cooperativity is temperature dependent, we collected data for the binding of GCA at five temperatures: 15, 20, 25, 30, and 37 °C. While a similar biphasic pattern is present at all temperatures, the data collected at higher temperatures display a more prominent first step in the binding isotherm. These differences result from differential macroscopic cooperativity at different temperatures. As can be seen in Table 2, the Hill coefficient decreases with increasing temperature. However, the binding of GCA remains highly cooperative at all temperatures examined.

**Synthesis of Extended Bile Salts.** In all of the natural bile salts evaluated, a hydrogen bond donor and acceptor resides at C-24. Therefore, it is difficult to determine which specific structural features of the bile salt side chain may play a role in recognition and cooperativity. To test whether this C-24 functionality is necessary for recognition and/or cooperativity, a panel of non-native side-chain-extended bile salts

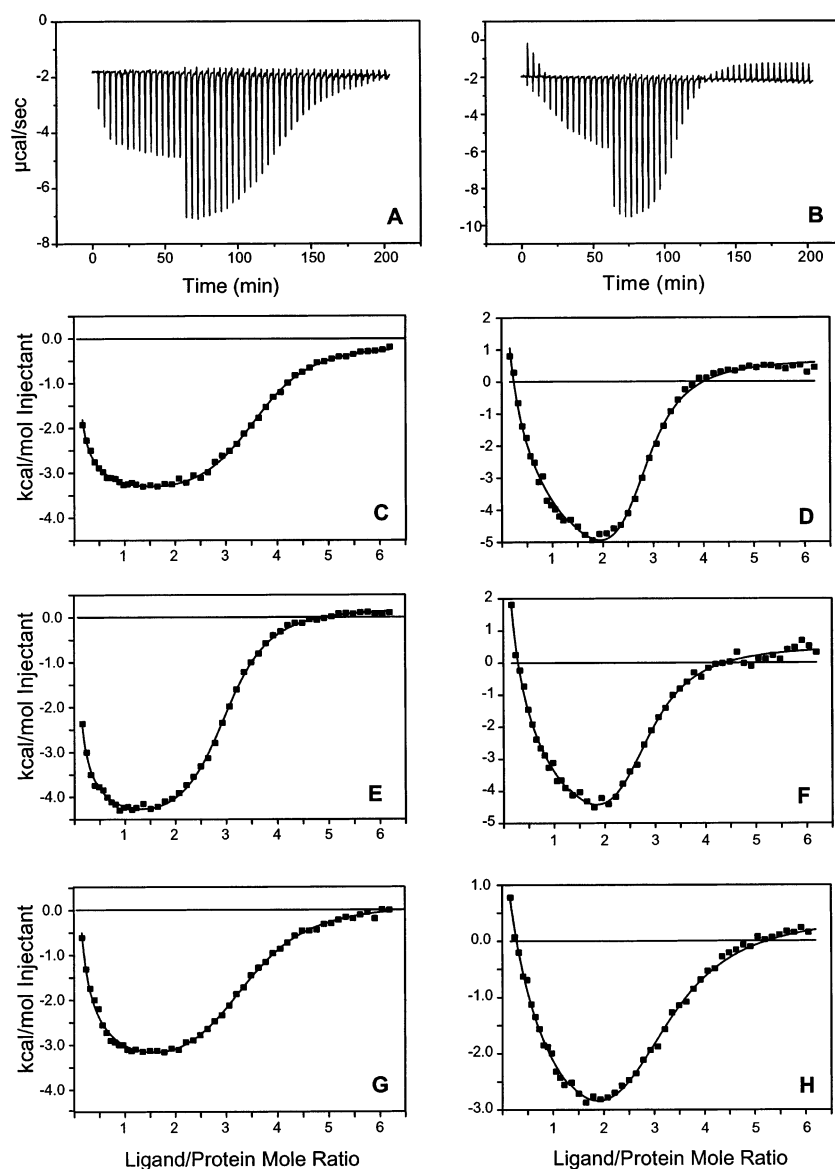


FIGURE 2: Isothermal titration calorimetry results for the binding of cholic acid and chenodeoxycholic acid derivatives to human I-BABP. Shown are the raw data, as injection profiles, for taurocholic acid (A) and taurochenodeoxycholic acid (B) and least-squares fitted isotherms for taurocholic acid (C), taurochenodeoxycholic acid (D), glycocholic acid (E), glycochenodeoxycholic acid (F), cholic acid (G), and chenodeoxycholic acid (H). The discontinuity at an  $x$ -axis value of approximately 60 min of the raw data represents a change in the injection volume from 4 to 7  $\mu\text{L}$ . The curve through the points represents a least-squares fit of the raw data using the two-step binding model defined in Materials and Methods.

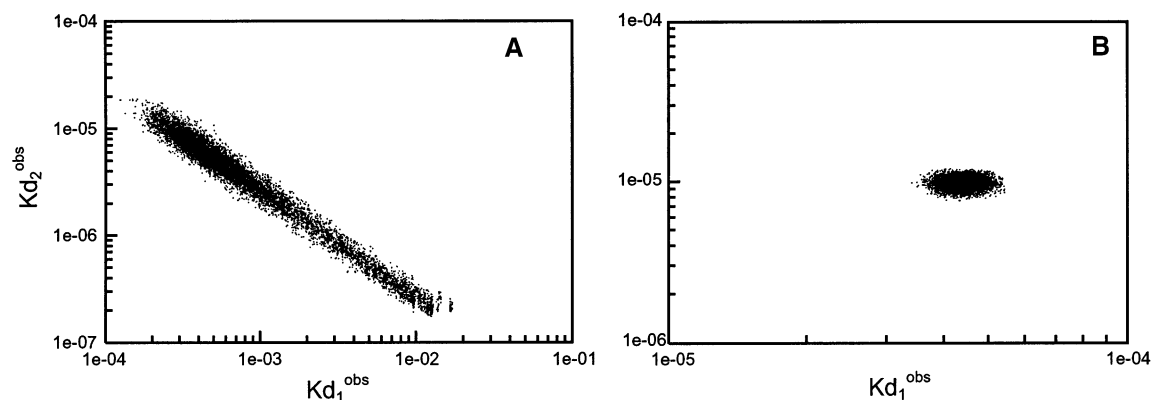


FIGURE 3: Bayesian analysis of the probability distribution for the fitted stepwise dissociation constants for taurocholic acid (A) and taurochenodeoxycholic acid (B) binding to human I-BABP at 25  $^{\circ}\text{C}$ .

was synthesized. By extending the side chain by two methylene units, we could effectively disrupt potential

protein–bile salt hydrogen bonding interactions occurring at the C-24 amide in conjugated bile salts, or the C-24 acid

Table 1: Stepwise Binding Parameters for the Interactions of Physiologically Relevant Bile Salts with Human Ileal Bile Acid Binding Protein at 25 °C<sup>a</sup>

bile salt	$K_{d1}^{obs}$ (M)	$K_{d2}^{obs}$ (M)	$\Delta H_1^{o,obs}$ (cal/mol)	$\Delta H_2^{o,obs}$ (cal/mol)	Hill coeff <sup>b</sup>
CA	$4.6 (\pm 1.7) \times 10^{-4}$	$2.6 (\pm 6.0) \times 10^{-6}$	$9.8 (\pm 8.7) \times 10^2$	$-1.2 (\pm 0.1) \times 10^4$	$1.86 (\pm 0.08)$
GCA	$4.9 (\pm 1.1) \times 10^{-4}$	$4.3 (\pm 1.2) \times 10^{-6}$	$3.3 (\pm 2.9) \times 10^3$	$-1.2 (\pm 0.04) \times 10^4$	$1.82 (\pm 0.04)$
TCA	$1.9 (\pm 3.0) \times 10^{-3}$	$4.6 (\pm 3.3) \times 10^{-6}$	$1.1 (\pm 2.2) \times 10^4$	$-8.6 (\pm 0.4) \times 10^3$	$1.91 (\pm 0.06)$
CDA	$7.6 (\pm 1.3) \times 10^{-5}$	$3.7 (\pm 0.8) \times 10^{-5}$	$8.7 (\pm 2.5) \times 10^2$	$-1.0 (\pm 0.1) \times 10^4$	$1.14 (\pm 0.09)$
GCDA	$6.2 (\pm 0.6) \times 10^{-5}$	$1.5 (\pm 0.2) \times 10^{-5}$	$2.8 (\pm 5.0) \times 10^3$	$-1.2 (\pm 0.03) \times 10^4$	$1.34 (\pm 0.05)$
TCDA	$4.4 (\pm 0.3) \times 10^{-5}$	$9.8 (\pm 0.7) \times 10^{-6}$	$2.5 (\pm 0.2) \times 10^3$	$-1.3 (\pm 0.02) \times 10^4$	$1.36 (\pm 0.03)$
DCA	$1.6 (\pm 8.8) \times 10^{-4}$	$4.6 (\pm 17.0) \times 10^{-5}$	$2.7 (\pm 5.4) \times 10^4$	$-6.5 (\pm 0.3) \times 10^4$	$1.30 (\pm 0.18)$
GDA	$9.2 (\pm 1.6) \times 10^{-5}$	$1.5 (\pm 2.8) \times 10^{-5}$	$-4.9 (\pm 2.1) \times 10^2$	$-6.9 (\pm 0.4) \times 10^3$	$1.42 (\pm 0.07)$
TDA	$3.6 (\pm 0.5) \times 10^{-5}$	$1.1 (\pm 0.1) \times 10^{-5}$	$-1.7 (\pm 0.1) \times 10^3$	$-9.4 (\pm 0.2) \times 10^3$	$1.29 (\pm 0.05)$

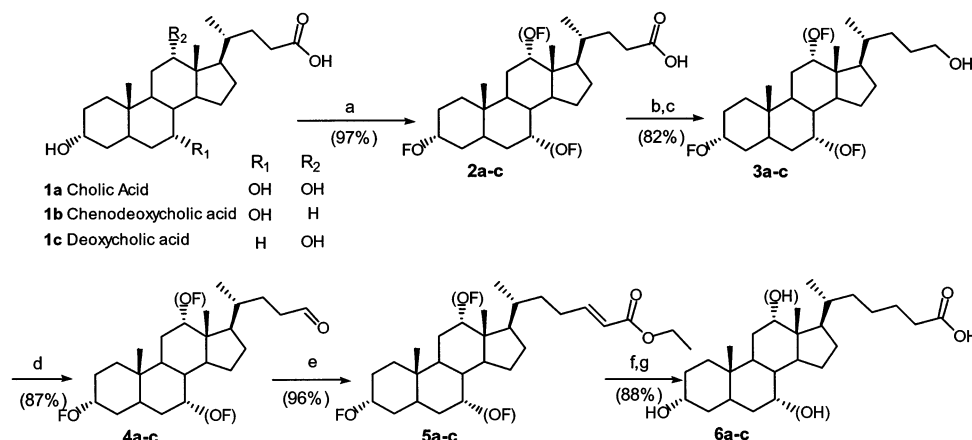
<sup>a</sup> The protein and ligand were dissolved in identical buffers containing 20 mM potassium phosphate, 135 mM KCl, and 10 mM NaCl, pH 7.2.

<sup>b</sup> The Hill coefficient, a commonly used measure of macroscopic cooperativity, varies from limiting values of 0–2 for extremely negatively and positively cooperative systems, respectively. It assumes a value of 1 for a noncooperative system. The Hill coefficient at half-saturation is related to the stepwise binding parameters as follows:  $n_H = 2/[1 + (K_{d2}^{obs}/K_{d1}^{obs})^{1/2}]$ .

Table 2: Stepwise Binding Parameters for Binding of Glycocholate to Human Bile Acid Binding Protein at Different Temperatures<sup>a</sup>

temp (°C)	$K_{d1}^{obs}$ (M)	$K_{d2}^{obs}$ (M)	$\Delta H_1^{o,obs}$ (cal/mol)	$\Delta H_2^{o,obs}$ (cal/mol)	Hill coeff <sup>a</sup>
15	$6.5 (\pm 0.6) \times 10^{-2}$	$8.1 (\pm 1.4) \times 10^{-8}$	$5.0 (\pm 0.6) \times 10^5$	$-8.6 (\pm 0.03) \times 10^3$	$1.998 (\pm 0.001)$
20	$9.6 (\pm 0.8) \times 10^{-2}$	$1.1 (\pm 1.6) \times 10^{-7}$	$5.0 (\pm 0.5) \times 10^5$	$-1.2 (\pm 0.1) \times 10^4$	$1.998 (\pm 0.001)$
25	$4.9 (\pm 0.3) \times 10^{-4}$	$4.3 (\pm 0.2) \times 10^{-6}$	$3.3 (\pm 0.6) \times 10^3$	$-1.2 (\pm 0.02) \times 10^4$	$1.82 (\pm 0.04)$
30	$4.4 (\pm 0.3) \times 10^{-4}$	$6.1 (\pm 0.2) \times 10^{-6}$	$2.5 (\pm 0.6) \times 10^3$	$-1.5 (\pm 0.03) \times 10^4$	$1.78 (\pm 0.04)$
37	$1.2 (\pm 1.2) \times 10^{-3}$	$8.6 (\pm 0.4) \times 10^{-6}$	$8.4 (\pm 1.8) \times 10^3$	$-2.0 (\pm 0.03) \times 10^4$	$1.84 (\pm 0.07)$

<sup>a</sup> See Table 1 for a definition of the Hill coefficient and sample conditions.

Scheme 1<sup>a</sup>

<sup>a</sup> Reagents and conditions: (a) formic acid,  $\text{HClO}_4$ ; (b) ethyl chloroformate,  $\text{Et}_3\text{N}$ , THF; (c)  $\text{NaBH}_4$ ,  $\text{H}_2\text{O}$ ; (d) PCC; (e) (carboethoxymethylene)triphenylphosphorane; (f) Pd/C,  $\text{H}_2$ ; (g) KOH, EtOH. Abbreviations: **6a**, eCA; **6b**, eCDA; **6c**, eDCA.

in unconjugated bile salts, but still retain the majority of the physical characteristics of the bile salts.

Our approach to synthesizing these compounds is shown in Scheme 1. We began with either cholic acid **1a** (3 $\alpha$ ,7 $\alpha$ ,12 $\alpha$ -trihydroxycholan-20-ic acid), chenodeoxycholic acid **1b** (3 $\alpha$ ,7 $\alpha$ -dihydroxycholan-20-ic acid), or deoxycholic acid **1c** (3 $\alpha$ ,12 $\alpha$ -dihydroxycholan-20-ic acid) and protected the ring hydroxyls as formyl esters **2a–c** using the Tserng methodology (14). The reduction of the C-24 carboxylic acid is achieved by first converting the acid to the mixed anhydride formed with ethyl chloroformate, which is then subsequently reduced with sodium borohydride. This afforded the C-24 alcohols **3a–c** which were readily oxidized to the C-24 aldehydes **4a–c** using pyridinium chlorochromate and further reacted with the commercially available Wittig reagent (carboethoxymethylene)triphenylphosphorane to afford the  $\alpha,\beta$ -unsaturated esters **5a–c**. Hydrogenation and saponification yielded the side-chain extended bile salts **6a–c**. This synthetic route proved to be very efficient, as the overall

yield was greater than 50% over seven steps. Although the methodology presented was applied only to CA, CDA, and DCA, it would be applicable to most cholanic acids.

The binding parameters for these compounds are provided in Table 3. These compounds exhibited the same calorimetric and energetic profile as the naturally occurring bile salts in that extended cholic acid (eCA) displayed the highest degree of macroscopic cooperativity of the three extended bile salts. The overall affinities and cooperativity for all three bile salts were similar to their naturally occurring counterparts, indicating that potential pairwise interactions involving C-24 were not critical for recognition or cooperativity.

**Binding of Bile Salt Mixtures.** Under physiologic conditions, I-BABP would encounter a heterogeneous pool of ligand substrates leading to a diverse collection of protein–ligand complexes. To begin to address the binding energetics of such systems, we tested mixtures of the three physiologically most abundant bile salts in their glycine-conjugated form. The binding parameters for these mixed systems are



Table 3: Stepwise Binding Parameters for the Interactions of Side-Chain-Extended Bile Salts with Human Ileal Bile Acid Binding Protein at 25 °C<sup>a</sup>

bile salt	$K_{d1}^{obs}$ (M)	$K_{d2}^{obs}$ (M)	$\Delta H_1^{obs}$ (cal/mol)	$\Delta H_2^{obs}$ (cal/mol)	Hill coeff <sup>a</sup>
eCA	$1.4 (\pm 0.4) \times 10^{-4}$	$4.2 (\pm 0.9) \times 10^{-6}$	$2.4 (\pm 1.4) \times 10^3$	$-8.3 (\pm 0.1) \times 10^3$	$1.70 (\pm 0.06)$
eCDA	$1.9 (\pm 0.3) \times 10^{-5}$	$2.0 (\pm 0.4) \times 10^{-5}$	$6.6 (\pm 0.2) \times 10^3$	$1.8 (\pm 0.2) \times 10^3$	$0.99 (\pm 0.08)$
eDCA	$1.5 (\pm 0.5) \times 10^{-4}$	$2.4 (\pm 0.9) \times 10^{-5}$	$-1.0 (\pm 0.2) \times 10^3$	$-4.6 (\pm 0.4) \times 10^3$	$1.43 (\pm 0.14)$

<sup>a</sup> See Table 1 for a definition of the Hill coefficient and sample conditions.Table 4: Stepwise Binding Parameters for the Interactions of 1:1 Mixtures of Glycine-Conjugated Bile Salts with Human Ileal Bile Acid Binding Protein at 25 °C<sup>a</sup>

bile salt mixture	$K_{d1}^{obs}$ (M)	$K_{d2}^{obs}$ (M)	$\Delta H_1^{obs}$ (cal/mol)	$\Delta H_2^{obs}$ (cal/mol)	Hill coeff <sup>a</sup>
GCA•GCDA	$1.3 (\pm 0.1) \times 10^{-4}$	$5.2 (\pm 0.5) \times 10^{-6}$	$7.0 (\pm 4.2) \times 10^2$	$-1.4 (\pm 0.1) \times 10^4$	$1.67 (\pm 0.02)$
GCA•GDA	$2.0 (\pm 0.6) \times 10^{-4}$	$7.6 (\pm 1.9) \times 10^{-6}$	$6.7 (\pm 0.1) \times 10^3$	$-9.5 (\pm 0.2) \times 10^3$	$1.67 (\pm 0.07)$
GCDA•GDA	$5.7 (\pm 1.2) \times 10^{-5}$	$1.6 (\pm 0.2) \times 10^{-5}$	$1.0 (\pm 0.7) \times 10^3$	$-1.2 (\pm 0.1) \times 10^4$	$1.30 (\pm 0.08)$

<sup>a</sup> See Table 1 for a definition of the Hill coefficient and sample conditions.

shown in Table 4. When comparing these systems to the homotypic complexes of Table 1, note that the energetic parameters for the mixed systems seem to be averages of the individual constituents. Of particular interest are the two systems that contain GCA. When GCA is mixed with either GCDA or GDA, the binding isotherms appear to be similar to those of GCA alone, but the affinity constants and Hill coefficients seem to reflect averages of the values between the corresponding homotypic systems.

## DISCUSSION

All bile salts studied in this analysis bound to I-BABP with similar overall affinity as reflected by the products of the  $K_{d1}^{obs}$  and  $K_{d2}^{obs}$ . However, the degree of macroscopic cooperativity varied significantly depending on the hydroxylation pattern of the bile salt. Bile salts derived from cholic acid displayed the highest degree of positive cooperativity. This effect was seen in both conjugated and unconjugated bile salts in addition to bile salts with a synthetically extended side chain. Further, this cooperativity was seen at all temperatures and even when mixtures of bile salts were used as the binding substrate.

The averaging effects that we observed in the mixed systems could be explained several ways. For example, the intrinsic affinity for binding of the first molecule of bile salt could be similar over all of the bile salts. Taking the example of the GCDA and GCA mixed system, either GCA or GCDA could bind to form singly ligated complexes. Then the singly ligated complexes which have GCA bound would demonstrate a large amount of cooperativity for binding of the second ligand, while the singly ligated complexes with GCDA bound would have a much lower degree of cooperativity for binding of the second ligand, thus leading to averaging of the overall macroscopic cooperativity.

These energetic patterns for the recognition of bile salts by I-BABP have implications for its biological function. Most other members of the intracellular lipid binding protein family bind a single fatty acid or retinoid molecule with nanomolar affinity (1). This high binding affinity is generally thought to be associated with a targeted delivery function for the protein. The binding properties for human I-BABP, which binds two molecules of bile salt with weak intrinsic affinity but positive cooperativity, are distinctly different. This distinction is suggestive of a fundamentally different

role for I-BABP. This protein is abundant in the absorptive epithelial cells located in the distal small intestine and has been previously implicated in the transcytoplasmic transport of bile salts in the context of their enterohepatic circulation. Because of the modest affinity, a sizable fraction of the bile salts can remain unbound at low bile salt concentrations. This could permit a significant flux of bile acid through the enterocyte as unbound monomers. Compared with retinoids and fatty acids, bile acids have much higher monomer solubility and may not need a protein carrier to traverse the cytoplasm. However, because of their inherent detergent activity, bile salts have the potential to cause damage in the cells through micelle formation. This could possibly be the mechanism underlying bile salt induced apoptosis. Both DCA and CDA family members have been previously shown to induce apoptosis whereas CA derivatives display reduced toxicity (15–17). It is then curious that both DCA and CDA derivatives bind with lower degrees of cooperativity but similar overall affinity when compared to CA derivatives. Because the partitioning of binding energies between intrinsic affinity and cooperativity differs between bile salt family members, I-BABP will bind CDA and DCA derivatives at lower bile salt concentrations as compared to CA derivatives. Perhaps I-BABP has evolved to selectively buffer DCA and CDA derivatives at lower concentrations as compared to CA derivatives to protect enterocytes from their increased toxicity.

Alternatively, I-BABP could potentially be playing a feedback role in FXR regulation. Previously, FXR has been shown to transcriptionally regulate  $7\alpha$ -hydroxylase, the rate-limiting step in bile salt synthesis, and I-BABP. When bile salts were bound to FXR, the expression of  $7\alpha$ -hydroxylase was repressed while the expression of I-BABP was activated. Of the bile salts examined in this study, CDA and DCA were shown to significantly activate the FXR receptor while CA derivatives were not (8). It is possible that the differential energetics of bile salt binding to I-BABP play a role in this feedback loop.

The structural correlates of the cooperative energetics for bile salt binding to I-BABP are not yet clear. There could be an allosteric interaction that leads to the observed cooperativity, where the binding of the first ligand is energetically communicated to the second site through a conformational change in the protein. Alternatively, the

binding of the first bile salt may provide a favorable binding surface for the second through a direct ligand–ligand interaction. Either of these models could be used to create an explanation for the bile salt dependence of cooperativity. GCA, which is the only bile steroid conjugate containing hydroxyl groups for hydrogen bond interactions involving both the B- and C-rings, may be better able to effect a conformational change in the protein, increasing the affinity for the second ligand. Conversely, GCA itself may simply present a more favorable surface for the binding of the second ligand. The three-dimensional structure of a doubly ligated complex should help to distinguish between these possibilities.

#### SUPPORTING INFORMATION AVAILABLE

Detailed experimental methodology for the synthesis of side-chain elongated bile salts. This material is available free of charge via the Internet at <http://pubs.acs.org>.

#### REFERENCES

1. Glatz, J. F., and van der Vusse, G. J. (1996) *Prog. Lipid Res.* 35, 243–282.
2. Veerkamp, J. H., and Maatman, R. G. (1995) *Prog. Lipid Res.* 34, 17–52.
3. Lin, M. C., Kramer, W., and Wilson, F. A. (1990) *J. Biol. Chem.* 265, 14986–14995.
4. Sacchettini, J. C., Hauft, S. M., Van Camp, S. L., Cistola, D. P., and Gordon, J. I. (1990) *J. Biol. Chem.* 265, 19199–19207.
5. Miller, K. R., and Cistola, D. P. (1993) *Mol. Cell. Biochem.* 123, 29–37.
6. Tochtrop, G. P., Richter, K., Tang, C., Toner, J. J., Covey, D. F., and Cistola, D. P. (2002) *Proc. Natl. Acad. Sci. U.S.A.* 99, 1847–1852.
7. Small, D. M., Dowling, R. H., and Redinger, R. N. (1972) *Arch. Intern. Med.* 130, 552–573.
8. Makishima, M., Okamoto, A. Y., Repa, J. J., Tu, H., Learned, R. M., Luk, A., Hull, M. V., Lustig, K. D., Mangelsdorf, D. J., and Shan, B. (1999) *Science* 284, 1362–1365.
9. Thompson, J., Winter, N., Terwey, D., Bratt, J., and Banaszak, L. (1997) *J. Biol. Chem.* 272, 7140–7150.
10. Bortolini, O., Medici, A., and Poli, S. (1997) *Steroids* 62, 564–577.
11. Wiseman, T., Williston, S., Brandts, J. F., and Lin, L. N. (1989) *Anal. Biochem.* 179, 131–137.
12. Johnson, B. H., and Hecht, M. H. (1994) *Bio/Technology* 12, 1357–1360.
13. Pace, C. N., Vajdos, F., Fee, L., Grimsley, G., and Gray, T. (1995) *Protein Sci.* 4, 2411–2423.
14. Tserng, K.-Y., and Klein, P. D. (1977) *Steroids* 29, 635–648.
15. Garewal, H., Bernstein, H., Bernstein, C., Sampliner, R., and Payne, C. (1996) *Cancer Res.* 56, 1480–1483.
16. Pritchard, D. M., and Watson, A. J. (1996) *Pharmacol. Ther.* 72, 149–169.
17. Sodeman, T., Bronk, S. F., Roberts, P. J., Miyoshi, H., and Gores, G. J. (2000) *Am. J. Physiol.* 278, 992–999.

BI0346502